Microstructure, hardness and cavitation erosion behaviour of Ti–6Al–4V laser nitrided under different gas atmospheres

J. Kaspar*[1], J. Bretschneider[1], S. Jacob[2], S. Bonß[1], B. Winderlich[1] and B. Brenner[1]

The present paper reports on a comparative study of the microstructure, hardness and cavitation erosion behaviour of Ti–6Al–4V laser nitrided under different gas atmospheres with nitrogen concentrations of 0–25%. By varying the nitrogen content of the gas atmosphere, the structure and hence the hardness and cavitation erosion behaviour of the laser nitrided layers can be controlled in a wide range. With increasing nitrogen content of the gas atmosphere, the structure within the laser nitrided layers characteristically changed from martensitic α'-Ti to a fine mixture of α- and β-Ti grains, finally leading to the formation of different titanium nitrides. The study revealed that the increase of hardness and cavitation erosion resistance can be mainly attributed to solid solution hardening of the nitrogen. It is shown that optimum cavitation erosion resistance is only achieved if crack free layers containing no brittle titanium nitrides are produced.

Keywords: Laser nitriding, Ti–6Al–4V, Cavitation erosion resistance, Microstructure

Introduction

Because of its high specific strength, excellent corrosion resistance and exceptional biocompatibility, titanium alloy Ti–6Al–4V has found various applications in aerospace, chemical industry, offshore, biomedicine, power generation, performance sports and automotive industry. Ti–6Al–4V, like other titanium alloys, is generally characterised by poor tribological properties so that the use of this alloy has been mainly restricted to non-tribological applications. To improve the tribological properties of Ti–6Al–4V, especially its low wear resistance, different surface engineering techniques have been applied with more or less success.[1–3]

Among others, laser nitriding has proven to be one promising way to overcome the poor tribological behaviour of Ti–6Al–4V (Refs. 4–6). Laser nitriding involves the melting of metal surface in a nitrogen containing atmosphere. Owing to the strong affinity of the molten titanium to nitrogen, nitrogen is very rapidly picked up and distributed within the melt by convection and diffusion in the liquid state, leading to the formation of titanium nitrides during solidification. It has been shown in literature that deep wear resistant layers of up to 1·5 mm thickness, exhibiting hardnesses in the range of 500–1500 HV, could be achieved by laser nitriding of Ti–6Al–4V (Refs. 4–19). Depending on the processing parameters applied (nitrogen content of the gas atmosphere, gas flow, laser power, spot diameter, traverse speed, track overlap, beam mode), complex microstructures are developed in the melt pool.[5,6,12,20–27] From this work, it can be assumed that the laser nitrided layers consist of face centred cubic (fcc) titanium nitride (TiN$_X$, $0{\cdot}7 \geqslant X \leqslant 0{\cdot}85$), tetragonal (tet) titanium nitride (Ti$_2$N), hexagonal closed packed (hcp) titanium nitride (TiN$_{0{\cdot}3}$), hcp α titanium (α-Ti) and body centred cubic (bcc) β titanium (β-Ti). In previous work, the authors found that the nitrogen content of the gas atmosphere was a key processing parameter to influence the structure and the hardness of the laser nitrided layers.[26,27] Laser remelting under a pure argon atmosphere and laser nitriding under a gas atmosphere containing 20% nitrogen led to microstructures which were predominantly martensitic α'-Ti and hcp α-Ti and respectively, containing only a few or no titanium nitrides. In contrast, laser nitriding under a gas atmosphere containing 40 and 80% nitrogen produced microstructures mainly consisting of plate-like shaped TiN$_{0{\cdot}3}$ and dendritic TiN$_X$ respectively.

Damage due to cavitation and water droplet erosion often occurs in titanium components such as pumps, impellers, high speed mixers, sonotrodes and steam turbine blades. The ability of laser nitriding to improve cavitation and water droplet erosion of Ti–6Al–4V has been shown in a few publications.[10–12,18,19,28,29] By this work, it became clear that a surface hardness in the range from 400 to ~800 HV was suitable to significantly enhance the erosion resistance of Ti–6Al–4V. This is in contrast to abrasive and sliding wear protection, where very high surface hardnesses are required.[10,17,18] To achieve such moderate hardnesses, the laser nitriding can be conducted under diluted gas atmospheres containing nitrogen less than ~50%. However, up to

[1]Fraunhofer-Institut für Werkstoff- und Strahltechnik Dresden, Winterbergstr. 28, D–01277 Dresden, Germany
[2]Technische Universität Dresden, D–01062 Dresden, Germany

*Corresponding author, email joerg.kaspar@iws.fraunhofer.de

now no systematic information exists about the correlation of microstructure, hardness and erosion behaviour for such processing conditions. Hence, in the present work, samples of Ti–6Al–4V were laser nitrided using a CO_2 laser and mixtures with nitrogen/argon ratio below 1 : 3. The hardness and microstructure of the laser nitrided layers were investigated by metallographic and electron microscopic methods. In addition, the cavitation erosion behaviour of the samples in deionised water was studied before and after the laser nitriding.

Experimental techniques

Specimens and laser treatment

In the present work, the $(\alpha + \beta)$ titanium alloy Ti–6Al–4V with the following composition was used: Ti–6·4Al–4·1V–0·19Fe–0·156O–0·007C–0·007N (wt-%). Specimens 60×40 mm with 6 mm thickness were laser nitrided, utilising a 6 kW cw CO_2 laser. Sets of 45 overlapping tracks were laser processed, using mixtures with nitrogen/argon ratio in the range from 0 : 100 to 25 : 75. To ensure a fine adjustment as well as oxygen free gas atmosphere, a bell shaped inert gas device was used, which had been developed previously.[17,30] The laser nitriding was conducted, using 3·1 kW laser power, 3·5 mm spot diameter, 9 mm s^{-1} traverse speed, 2·75 mm track overlap and a constant gas flow of 100 L min^{-1}.

Characterisation methods

The microstructural changes which occur during laser nitriding of Ti–6Al–4V were examined by different methods. First, the specimen surface was examined by scanning electron microscopy (SEM). Then cross-sections of the layers were prepared by grinding and polishing. The polished specimens were chemically etched in a solution of 2 mL HF, 2 mL HNO_3 and 96 mL H_2O for a period of $\sim$20 s. A Leica MeF4 optical microscope was used for standard metallographic characterisation. Further information about the structure and the spatial distribution of the phases formed was obtained by SEM using secondary and backscattered electrons as well as energy dispersive X-ray spectroscopy (EDS). Moreover, the hardnesses of the nitrided layers were measured at cross-sections by means of a Vickers microhardness tester using a 100 g load.

An ultrasonic induced cavitation device was used to carry out the cavitation erosion tests in deionised water at 25°C (ASTM G32-92). The specimen was set opposite to a vibrating tip of Ti–6Al–4V. Cavitation was induced by longitudinal oscillation at 20 kHz at an amplitude of 40 µm and a distance of 0·50 mm between tip and sample. Before testing, the samples were cut and surface ground. The mass loss was determined at specific intervals during a total testing of 20 h exposure to cavitation with an accuracy of 0·1 mg. To convert the mass loss into volume loss, it was divided by the density of Ti–6Al–4V. After testing, the surface and cross-sections of the eroded samples were examined by SEM in order to identify the predominate erosion mechanisms.

Results

Microstructure and hardness

Laser nitriding under gas atmospheres containing 0–25% nitrogen led to the formation of macrocrack free

layers of $\sim$0·5 mm thickness. Figures 1 and 2 demonstrate how the nitrogen content of the gas atmosphere affected the structural evolution in the laser nitrided areas. Remelting under a pure argon atmosphere completely destroyed the fine grained globular structure of the as delivered state, resulting in a solidification structure which consisted of large β-Ti grains with sizes ranging from 200 to 500 µm. During rapid cooling, the bcc crystal structure was completely switched to the hcp α' structure by a diffusionless martensitic transformation. As a consequence, acicular martensite is formed, the needles of which often extend all through the former β-Ti grains (Figs. 1a and 2a).

The microstructure within the laser processed layers is already noticeably changed if the gas atmosphere contained only a little nitrogen. Up to a nitrogen content of the gas atmosphere of $\sim$5%, the predominant structure which was found within the transformed β grains was still martensitic α'-Ti. However, the length of the martensite needles significantly decreased with increasing nitrogen content of the gas atmosphere until the martensitic transformation was completely suppressed. Accordingly, the transformation structure formed owing to laser processing under gas atmospheres containing 5–25% nitrogen mainly consisted of small α-Ti grains (Fig. 2b–d). It could be verified by EDS analysis that the small α-Ti grains were surrounded by vanadium rich areas. In accordance with previous work, these vanadium rich areas can be regarded as β-Ti (Ref. 27). It is noteworthy that α-Ti grains which formed along the grain boundaries of the former β-Ti grains were considerably larger and more elongated than those in the grain interior (Fig. 2b and c).

The solidification of separate nitrogen rich phases commenced at a nitrogen content of the gas atmosphere of $\sim$11%. These titanium nitrides exhibit globular and plate-like shapes respectively (Figs. 1c, d, 2c and d). A considerable amount of plate-like titanium nitrides were found in samples that had been laser nitrided under gas atmospheres containing 25% nitrogen. From results reported in literature[22–24] and TEM observations in previous studies by the authors,[26,27] it can be concluded that the globular and plate shaped phases are hcp $TiN_{0.3}$. In contrast, dendritic crystallisation of fcc TiN is characteristic of laser nitriding under gas atmospheres mainly containing nitrogen.[26,27] Therefore, TiN dendrites were only sparsely found in samples laser nitrided under a gas atmosphere containing 25% nitrogen.

It should be mentioned that a thin, continuous layer of titanium nitrides was found on the surface of all laser nitrided samples (Fig. 2). With increasing nitrogen content of the gas atmosphere, the thickness of this layer increased from several hundreds of nanometres to a few micrometres. It is important to note that this layer contains numerous microcracks.[26] It will be shown elsewhere by detailed TEM analysis that this layer consists of both fcc TiN and hcp $TiN_{0.3}$ (Ref. 31).

Figure 3 shows the measured mean microhardness of the laser nitrided layers and its dependence on the nitrogen content of the gas atmosphere. It is evident that the hardness strongly depends on the composition of the gas atmosphere, especially in the low nitrogen concentration range. While the remelting under pure argon atmosphere increased the hardness by $\sim$50 HV0·1 with respect to the as delivered state, there was a considerable
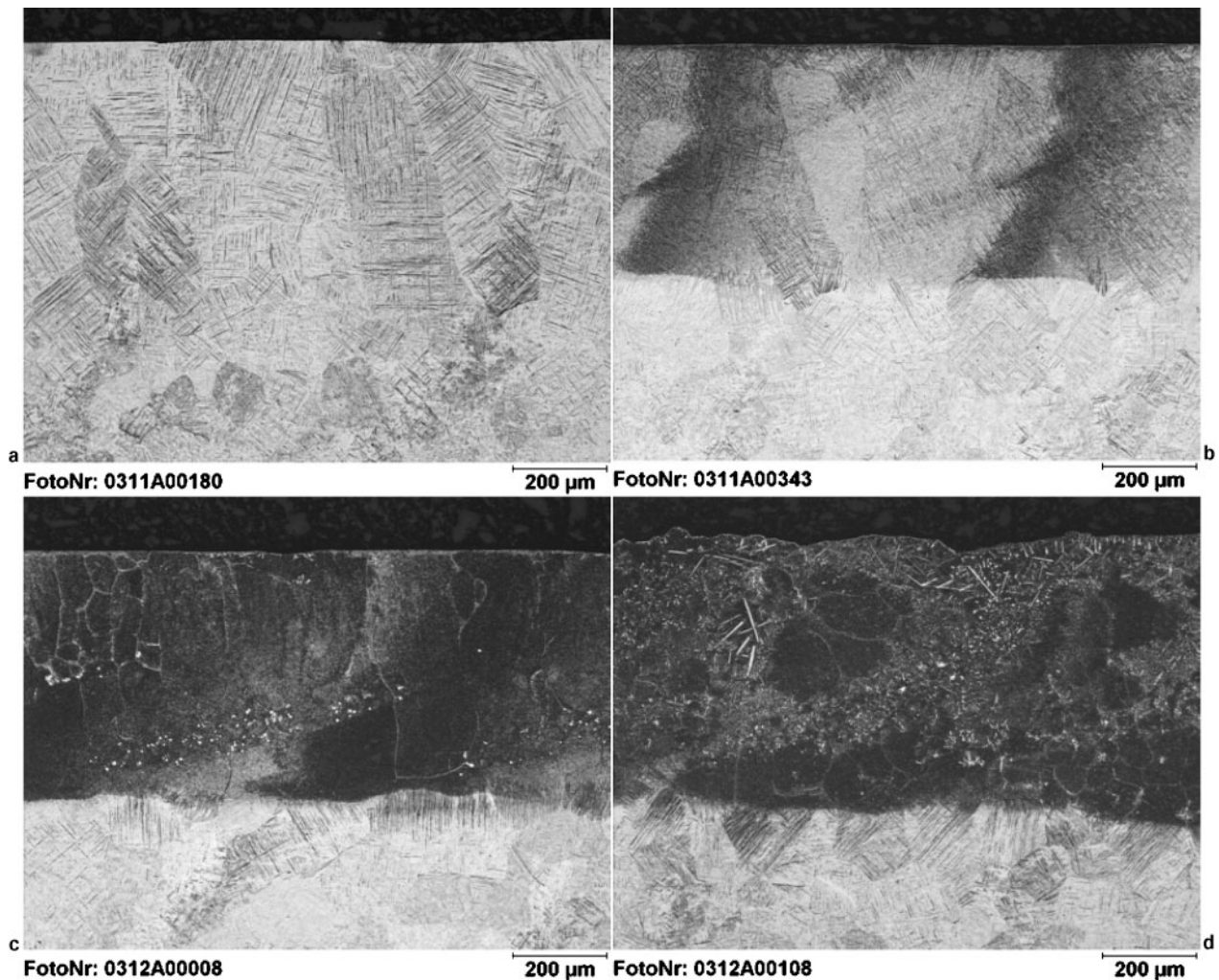
a laser remelted; *b* laser nitrided: N_2/Ar 5:95; *c* laser nitrided: N_2/Ar 13:87; *d* laser nitrided: N_2/Ar 25:75

1 Optical micrographs of cross-sections through specimens that were laser processed under different gas atmospheres: note changes in microstructure occurring with increasing nitrogen content of gas atmosphere and furthermore that in *a*, boundary between melt pool and heat affected zone (HAZ) is not visible

increase in hardness by laser nitriding under the gas atmosphere with nitrogen content in the range of 2–19%. Clearly, the hardness achieves a plateau at ~ 560 HV0·1. It should be furthermore mentioned that the hardness distribution through the laser nitrided layers was quite uniform independent of the composition of the gas atmosphere.

Cavitation erosion behaviour

In order to remove the thin, continuous layer of titanium nitrides on the surface of the laser treated samples and to provide similar surface conditions, all samples were mechanically surface ground before cavitation erosion testing. It should be pointed out that as a result of the grinding operation, occasional and frequent cracking was induced in samples laser nitrided under gas atmospheres containing 19 and 25% respectively. These cracks extended all through the laser nitrided layers and were not stopped until the boundary to the heat affected zone. The cracking due to the grinding operation demonstrates that the mechanical resistance and ductility of the samples was noticeably reduced if the laser nitriding was conducted under gas atmospheres containing >13% nitrogen. It will be proved elsewhere by acoustic emission analysis that the

existence of brittle phases like $TiN_{0·3}$ and TiN_x are responsible for the enhanced crack sensitivity of laser nitrided samples.[31]

The cumulative volume loss during cavitation erosion of Ti–6Al–4V in the as delivered and different laser processed states over a total time of 20 h is plotted in Fig. 4. For all conditions, there exist an incubation period without any measurable volume loss, a transition period, where the rate of erosion increased towards a maximum, and a steady state period, where the erosion commences with constant erosion rate. It was found that the duration of the incubation period depended on the structural state of Ti–6Al–4V (Table 1). Samples in the as delivered state and samples laser nitrided under gas atmospheres containing 25% nitrogen only showed a negligible incubation period. In contrast, the incubation time of the other laser processed samples was in the range of 1–2 h, slightly increasing with increasing nitrogen content of the gas atmosphere. The transition region during cavitation erosion was independent of the composition of the gas atmosphere in the range of 3–4 h, leading to a start of the steady state period after 4–6 h of testing.

Figure 4 and Table 1 demonstrate that owing to the laser processing under gas atmospheres containing
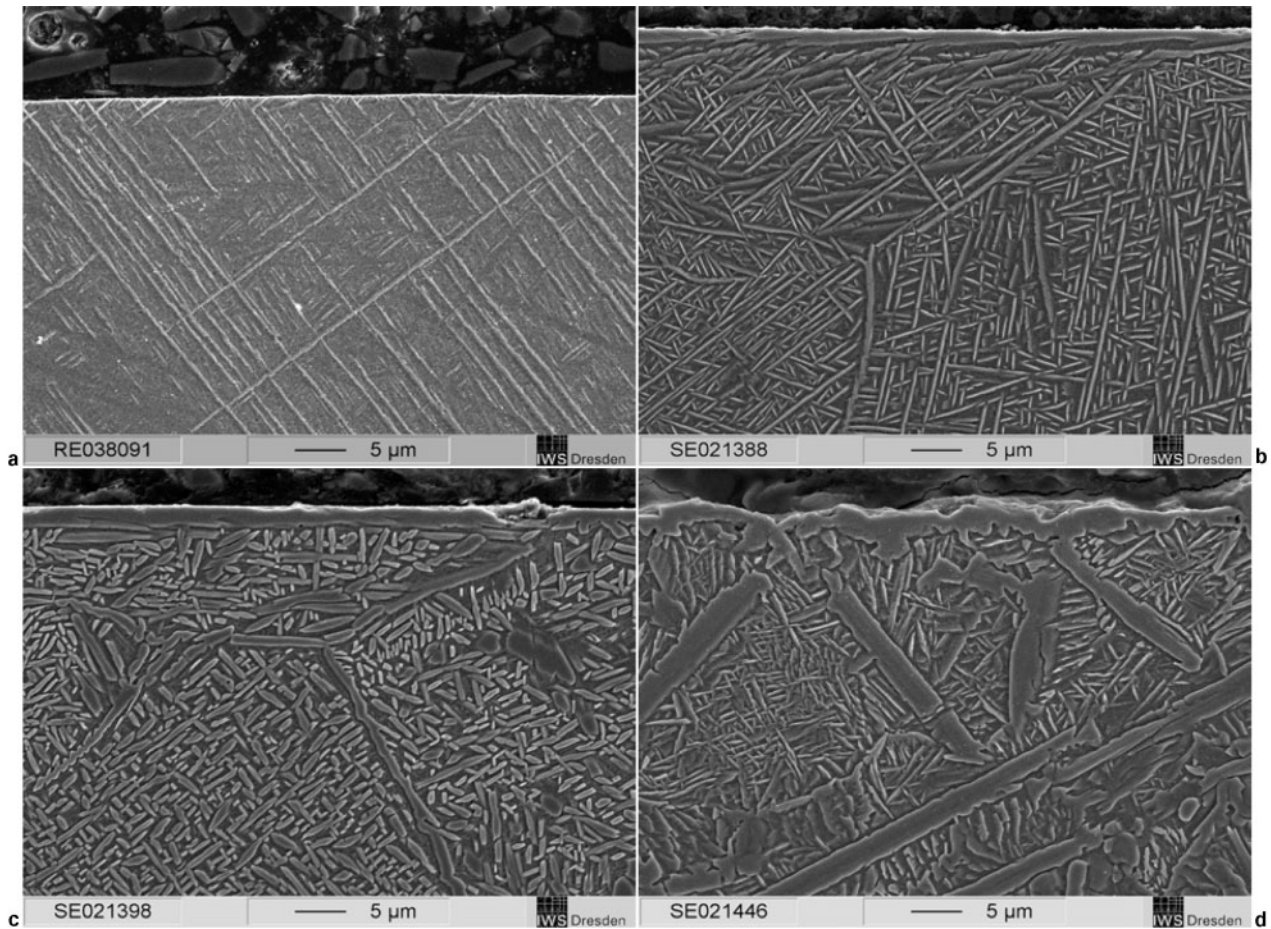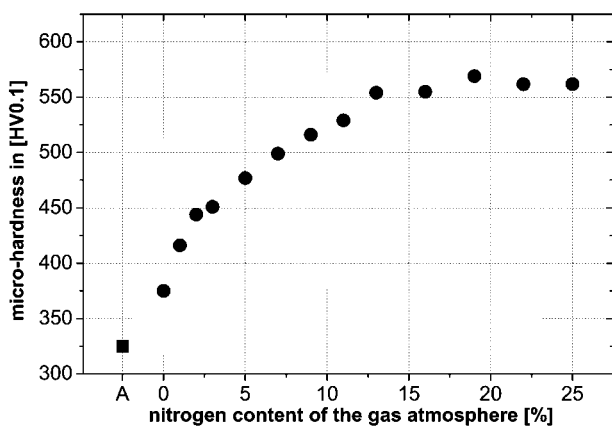
a laser remelted; *b* laser nitrided: N_2/Ar 5:95; *c* laser nitrided: N_2/Ar 13:87; *d* laser nitrided: N_2/Ar 25:75

2 Scanning electron microscopy images of cross-sections through specimens that were laser processed under different gas atmospheres: note changes in microstructure occurring with increasing nitrogen content of gas atmosphere

mixtures of different nitrogen/argon ratios, the cavitation erosion resistance of Ti–6Al–4 was considerably improved with respect to the as delivered state. Initially, the cumulative volume loss as well as the steady state erosion rate was distinctively reduced with increasing nitrogen content of the gas atmosphere but passed through a plateau in gas atmospheres containing >9% nitrogen. As a consequence, laser nitriding with gas atmospheres containing 9–25% nitrogen reduced both the cumulative volume loss and the steady state erosion rate to about one-third with respect to the as delivered state.

The dominant features of the erosion behaviour were rationalised by SEM observations of the surface and etched cross-sections of the eroded samples after 20 h of erosion (Figs. 5 and 6). Samples in the as delivered state exhibited a quite uniform eroded surface without preferential erosion pits and crater formation (Figs. 5a

3 Mean microhardness of laser nitrided layers in dependence on nitrogen content of gas atmosphere: for the sake of completeness, hardness of as delivered state (A) is included
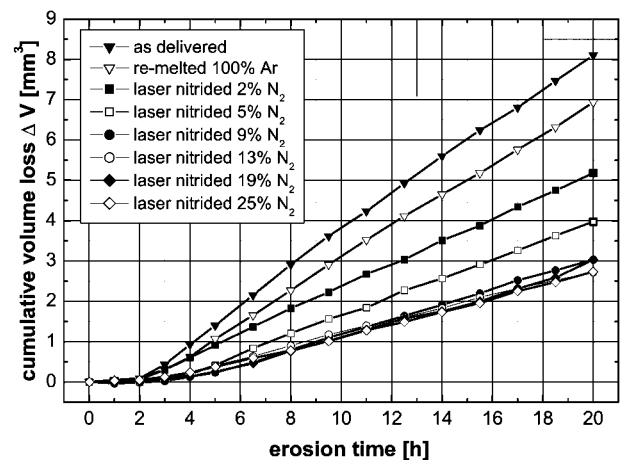
4 Cumulative volume loss during cavitation erosion test measured on samples in as delivered state and on samples in different laser processed states
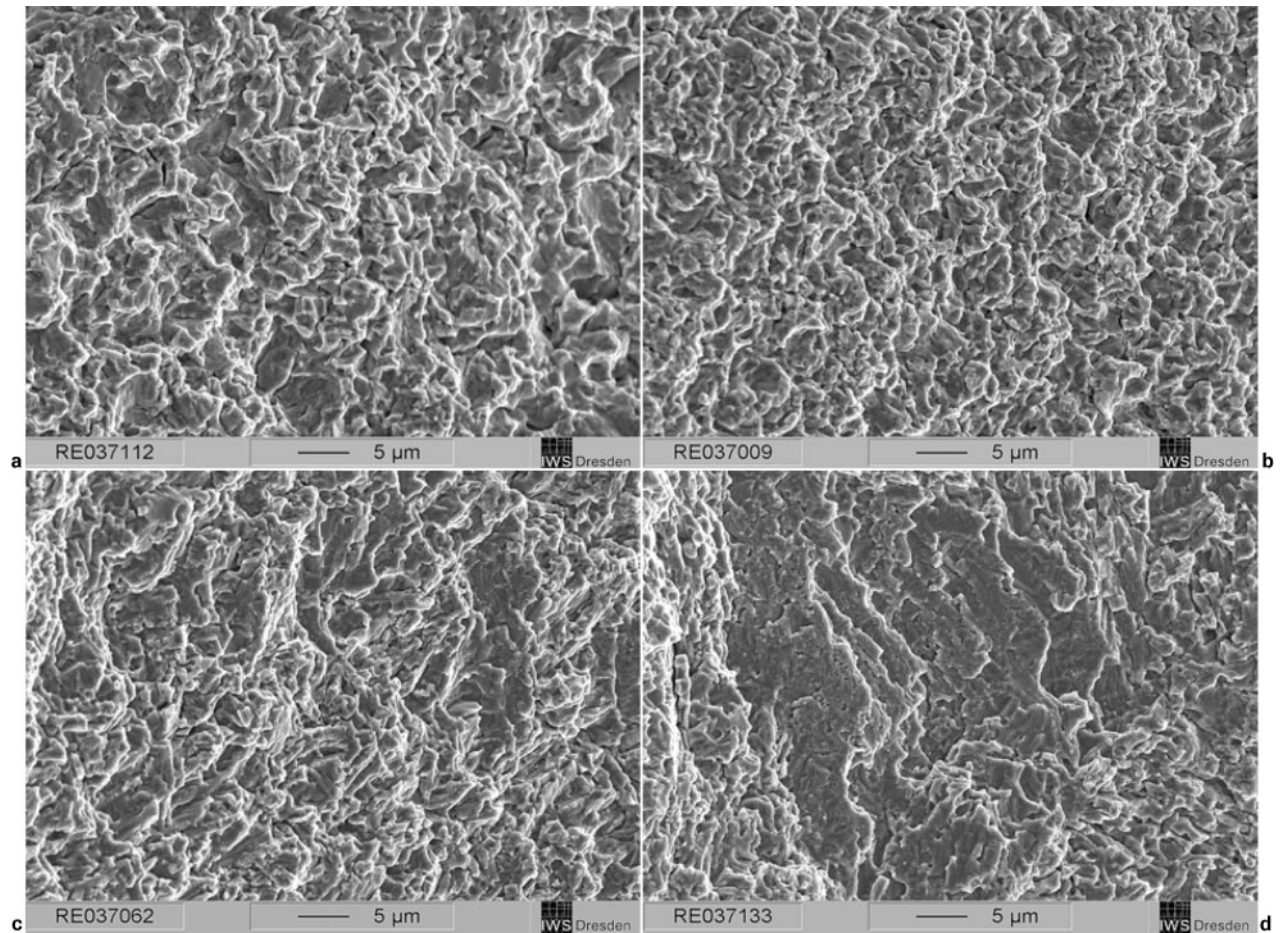
a as delivered; *b* laser nitrided: N₂/Ar 2:98; *c* laser nitrided: N₂/Ar 13:87; *d* laser nitrided: N₂/Ar 25:75
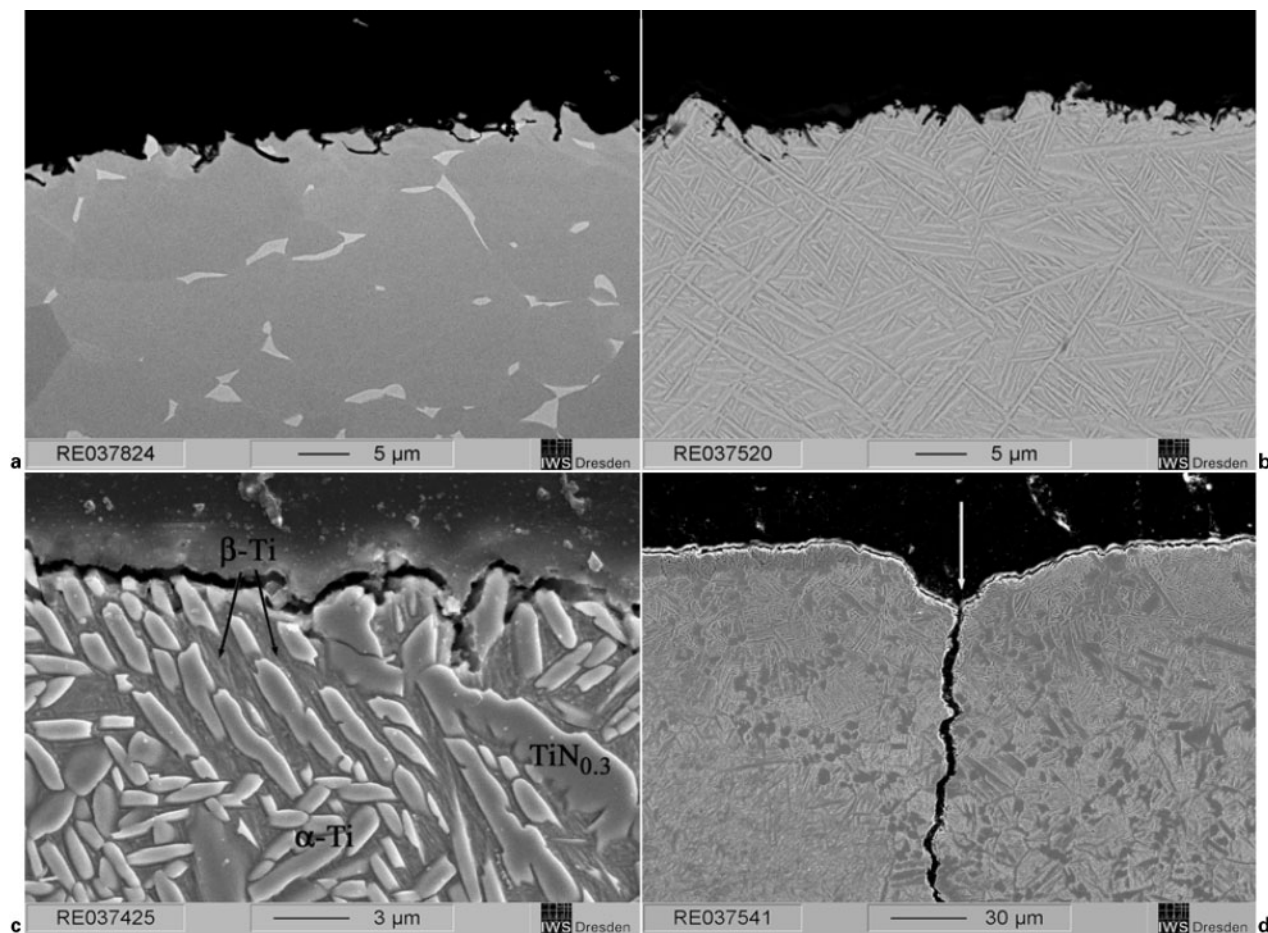**5 Scanning electron microscopy images of surface of eroded samples: note changes in surface morphology indicating transition from ductile fracture to brittle fracture failure**

and 6*a*). Moreover, it should be noted that the surface revealed distinct signs of plastic deformation and ductile fracture over the whole eroded surface. The morphology of the eroded surface did not evidently change in the case of laser remelted samples. Similarly, the material loss of samples laser nitrided under gas atmospheres only containing 2% nitrogen was dominated by evenly distributed ductile fracture (Fig. 5*b*). With increasing nitrogen content of the gas atmosphere, the erosion induced surface pits and grooves at first became slightly smoother, indicating the transition from ductile fracture to brittle fracture failure (Fig. 5*c*). On the other hand, selective erosion attack on a microscopic scale was already observed on samples laser nitrided under gas atmospheres containing 5% nitrogen. In some regions of these samples, the erosion proceeded notably faster along the boundaries of the martensite needles (Fig. 6*b*). The selective erosion attack even became more pronounced if the nitrogen content of the gas atmosphere increased. Figure 6*c* clearly shows that material in-between the small α-Ti grains, which in accordance with microstructural investigation mainly was β-Ti, was more rapidly eroded than the α-Ti grains themselves. It is also important to note that the erosion attack became macroscopically heterogeneous if the samples were laser nitrided under gas atmospheres containing 19 and 25% nitrogen. On one hand, an accelerated erosion was found in the vicinity of cracks (Fig. 6*d*). On the other hand, extended areas of the eroded surface exhibited a rather smooth appearance, indicating that the material removal of these areas was governed by brittle fracture and spallation (Fig. 5*d*).

Table 1 Compilation of cavitation erosion data measured on as delivered as well as laser remelted and laser nitrided (LN) samples of Ti–6Al–4V

	As delivered	Remelted 100%Ar	LN 2%N₂	LN 5%N₂	LN 9%N₂	LN 13%N₂	LN 19%N₂	LN 25%N₂
Incubation period, h	<1	1	1	2	2	2	2	<1
Transition period, h	0–4	1–5	1–5	2–5	2–6	2–6	2–6	0–4
Cumulative erosion loss after 20 h, mm³	8·10	6·93	5·13	3·97	3·03	2·72	3·03	2·73
Erosion rate in the steady state period, mm³ h⁻¹	0·447	0·388	0·298	0·234	0·188	0·154	0·180	0·158

a as delivered; *b* laser nitrided: N_2/Ar 5:95; *c* laser nitrided: N_2/Ar 19:81; *d* laser nitrided: N_2/Ar 25:75
6 Scanning electron microscopy images of cross-sections of eroded samples

Discussion

The results of the present study reveal that laser remelting and laser nitriding of Ti–6Al–4V under gas atmospheres containing 2–25% nitrogen produces complex microstructures in the solidified melt zone. Thereby, the nitrogen content of the gas atmosphere strongly determines the nature, volume fraction, morphology and distribution of the phases formed during solidification and solid state transition reactions. Up to now, it has been generally assumed that laser nitrided layers of Ti–6Al–4V consist of different titanium nitrides (hcp $TiN_{0.3}$, tet Ti_2N, fcc TiN_X) and a metallic matrix composed of martensitic α'-Ti (Refs. 5, 6, 12, 20–25). However, earlier work has already revealed that the metallic matrix can also be built up of α-Ti grains and a fine dispersion of α- and β-Ti in-between the α-Ti grains respectively.[26,27] In the present study, it has been established that up to a nitrogen content of 11% in the gas atmosphere, the melt merely solidifies in the bcc β-Ti structure. During cooling, the β-Ti transformed to α'-Ti by a diffusionless martensitic transformation if the nitrogen content of the gas atmosphere was below 5%. Under a gas atmosphere containing >5% nitrogen, the martensitic transformation did not occur and the β-Ti decomposed into mixture of α- and β-Ti grains. It is known from literature that in Ti–6Al–4V, the martensite start temperature M_s is $\sim 200°C$ below the beta transus temperature $T_{\beta \rightarrow \alpha}$ 996°C (Ref. 32). It is furthermore known from the binary system of Ti–N that nitrogen as

well as raising the solidification temperature also strongly increases $T_{\beta \rightarrow \alpha}$ (Ref. 33). If it is assumed that the presence of nitrogen in the titanium lattice reduces M_s, the difference between $T_{\beta \rightarrow \alpha}$ and M_s rapidly increases with increasing the amount of nitrogen dissolved in the lattice. Consequently, there is sufficient time for the progression of the β-Ti to α-Ti transformation before the start of the martensitic reaction is reached. Hence if the nitrogen concentration dissolved in the lattice reaches a critical level, owing to increasing the nitrogen content of the gas atmosphere during laser nitriding, the martensitic transformation is suppressed in accordance with the authors' observations.

The increase in hardness observed in samples laser processed under gas atmospheres containing mixtures of different argon/nitrogen ratios can be correlated with the structures formed within the laser nitrided layers. It is assumed that the increase in hardness of the laser remelted layers with respect to the as delivered state can be ascribed to an increase in dislocation density which is introduced by the martensitic transformation. In contrast, the increase of hardness in the laser nitrided layers is manly attributed to solid solution hardening of nitrogen interstitially dissolved in the α-Ti lattice since titanium nitrides are only sparsely formed during laser nitriding under gas atmospheres containing <25% nitrogen.

Laser remelting and laser nitriding have proven to be a promising way to improve the cavitation erosion resistance of Ti–6Al–4V (Refs. 10, 19 and 28). However,
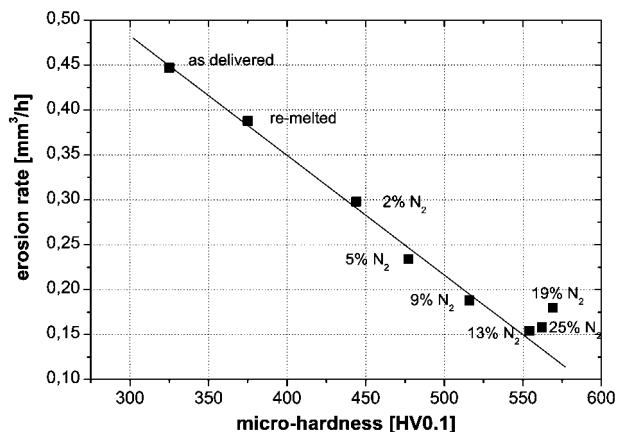
7 Correlation of erosion rate in steady state period of cavitation erosion test with average microhardness of as delivered state and different laser processed samples

up to now, only Robinson *et al.*[10] has clearly shown that the composition of the gas atmosphere during laser processing influences the cavitation erosion behaviour. They found that the cavitation erosion resistance of laser nitrided Ti–6Al–4V was slightly better if the gas atmosphere contained 10% instead of 20% nitrogen. They concluded that the augmented formation of cracks was responsible for this slightly surprising result. To the best of the authors' knowledge, in the present work, the first systematic study on the influence of the composition of gas atmosphere on the cavitation erosion behaviour of Ti–6Al–4V was undertaken. The results show that with increasing nitrogen content in the gas atmosphere, the volume loss and the steady state erosion rate of the laser nitrided samples continuously reduce to about one-third with respect to the as delivered state and saturate at a nitrogen content above 13% in the gas atmosphere. In Fig. 7, the steady state erosion rate is plotted against microhardness. It is remarkable that the erosion rate continuously decreases with hardness if the as delivered, laser remelted and laser nitrided states of up to 13% nitrogen content of the gas atmosphere are considered. However, the inversely proportional relationship between erosion rate and hardness no longer applies if samples laser nitrided under gas atmospheres containing 19 and 25% nitrogen are considered. The erosion rate of these samples does not further reduce even though their hardness still increases so that the erosion rate slightly deviates to higher values with respect to hardness.

Generally in metals, all metallurgical measures causing an enhancement of strength should also lead to an improvement of the cavitation erosion resistance unless the metal is too brittle to deform plastically.[34,35] According to Rieger,[34] the enhancement of both strength and cavitation erosion resistance is achieved by introducing obstacles to dislocation motion which improve the glide resistance of the dislocations within the crystal. However, in order to attain an optimal improvement of cavitation erosion resistance, these obstacles should be uniformly dispersed. In other words, the microstructure has to be as fine and homogenous as possible to achieve optimal cavitation erosion resistance. Also in the present work, the increase of erosion resistance in the laser processed samples can be ascribed to an enhancement of strength caused mainly by solid

solution hardening by nitrogen. However, beginning at a nitrogen content of 5% in the gas atmosphere, there develop structural in-homogeneities that prevent a further improvement of the cavitation erosion resistance with strength and hardness. First, differences in strength between, on the one hand β-Ti and on the other hand α-Ti and $TiN_{0.3}$, lead to a selective erosion attack which may accelerate the erosion process. These differences in strength develop with increasing nitrogen content dissolved in the lattice, owing to the solid solution hardening effect of the nitrogen, which occurs in α-Ti as well as in $TiN_{0.3}$ but not in β-Ti. As a consequence, the removal of the embedded harder phases α-Ti and $TiN_{0.3}$ is governed by the initial erosion of the softer β-Ti in-between and beside α-Ti and $TiN_{0.3}$. Second, the existence of cracks is obviously detrimental to the erosion resistance since the erosion propagates faster along the cracks than on the remaining surface areas. Finally, brittle fracture of phases like $TiN_{0.3}$ and TiN_X also promotes material loss during cavitation erosion. In this regard, it should be pointed out that the existence of cracks and titanium nitrides like $TiN_{0.3}$ and TiN_X are not only detrimental to cavitation erosion behaviour but can also be accounted for the degradation of fatigue strength and ductility of the laser nitrided samples as will be shown in a further publication.[31]

Conclusions

In the present work, the influence of the nitrogen content of the gas atmosphere in the range of 0–25% on the microstructure, hardness and cavitation erosion behaviour of laser nitrided Ti–6Al–4V has been thoroughly investigated. Based on the results of the present study, the following conclusions are drawn.

1. The nature, volume fraction and distribution of the phase formed during laser nitriding are strongly determined by the nitrogen content of the gas atmosphere. If the nitrogen content of the gas atmosphere is below 5%, the predominant microstructural feature is martensitic α'-Ti whereas laser nitriding under gas atmospheres containing >5% nitrogen mainly produces microstructures which consist of a fine mixture of α- and β-Ti grains. Increasing the nitrogen content of the gas atmosphere above 11% leads to the formation of globular and plate-like shaped $TiN_{0.3}$.

2. The increase of hardness in the laser nitrided layers is mainly attributed to solid solution hardening of the nitrogen.

3. The cavitation erosion resistance of the laser nitrided layers improves in a characteristic manner with the nitrogen content of the gas atmosphere. In order to achieve good erosion protection, uniform microstructures are essential. As long as the structure and the properties of the constituents are microscopically homogeneous, the improvement in erosion resistance can be ascribed to an overall increase in hardness and strength. In contrast, selective erosion attack induced by cracks or local strength differences limits the cavitation erosion resistance of the laser nitrided layers.

4. The optimum cavitation erosion resistance is readily achieved by laser nitriding under gas atmospheres containing comparatively small amounts of nitrogen. Under such gas atmospheres, crack free layers without any brittle titanium nitrides may be produced. These layers have the potential to endure high static

and cyclic stresses occurring during many technical applications.

Acknowledgements

References

1. P. H. Morton and T. Bell: Proc 6th World Conf. on 'Titanium', (ed. P. Lacombe *et al.*), les editions de physique, 1705–1712; Canne, France, June 1988, Société Francaise de Métallurgie.
2. A. Bloyce, H. Dong and B. Hanson: Proc. 8th World Conf. on 'Titanium', (ed. P. A. Blenkinsop *et al.*), 1975–1982; Birmingham, UK, October 1995, London, The Institute of Materials.
3. H. Dong and T. Bell: Proc. 10th World Conf. on 'Titanium', (ed. G. Lütjering and J. Albrecht), 867–874; Hamburg, Germany, July 2003, DGM/Wiley-VCH Verlag GmbH & Co. KGaA.
4. A. Walker, J. Folkes, W. M. Steen and D. R. F. West: *Surf. Eng.*, 1985, **1**, 23–29.
5. H. W. Bergmann: *Z. Werkstofftech.*, 1985, **16**, 392–405.
6. T. Bell, H. W. Bergmann, J. Lanagan, P. H. Morton and A. M. Staines: *Surf. Eng.*, 1986, **2**, 133–143.
7. J. P. Massoud and G. Coquerelle: Proc. 6th World Conf. on 'Titanium', (ed. P. Lacombe *et al.*), les editions de physique, 1847–1852; Canne, France, June 1988, Société Francaise de Métallurgie.
8. H. Xin and T. N. Baker: Proc. 8th World Conf. on 'Titanium', (ed. P. A. Blenkinsop *et al.*), 2031–2038; Birmingham, UK, October 1995, London, The Institute of Materials.
9. A. Weisheit and B. L. Mordike: *Surf. Eng.*, 1995, **11**, 160–161.
10. J. M. Robinson, S. Anderson, R. D. Knutsen and R. C. Reed: *Mater. Sci. Technol.*, 1995, **11**, 611–618.
11. J. M. Robinson and R. C. Reed: *Wear*, 1995, **186–187**, 360–367.
12. C. Gerdes, A. Karimi and H. W. Bieler: *Wear*, 1995, **186–187**, 368–374.
13. J. de Damborena, B. Fernàndez, V. Lòpez and A. J. Vàzques: *Int. J. Mater. Prod. Technol.*, 1996, **11**, 301–309.
14. J. E. Masse and J. F. Mathieu: *Mater. Manuf. Process.*, 1996, **11**, 207–214.
15. C. Hu and T. N. Baker: *J. Mater. Sci.*, 1997, **32**, 2821–2826.
16. S. Mridha and T. N. Baker: *J. Mater. Process. Technol.*, 1998, **77**, 115–121.
17. S. Bonß, B. Brenner and E. Beyer: *Mat.-wiss. Werkstofftech.*, 2001, **32**, 160–165.
18. S. Bonß, B. Brenner, H.-J. Scheibe and E. Beyer: Proc. 10th World Conf. on 'Titanium', 1001–1008; Hamburg, Germany, July 2003, DGM/Wiley-VCH Verlag GmbH & Co. KGaA.
19. H. C. Man, Z. D. Cui, T. M. Yue and F. T. Cheng: *Mater. Sci. Eng. A*, 2003, **A355**, 167–173.
20. C. Hu, S. Mridha, H. S. Ubhi, P. Holdway, A. W. Bowen and T. N. Baker: Proc. 8th World Conf. on 'Titanium', (ed. P. A. Blenkinsop *et al.*), 1959–1966; Birmingham, UK, October 1995, London, The Institute of Materials.
21. L. Xue, M. Islam, A. K. Koul, B. Bibby and W. Wallace: *Adv. Perform. Mater.*, 1997, **4**, 389–408.
22. C. Hu, H. Xin, L. M. Watson and T. N. Baker: *Acta Mater.*, 1997, **45**, 4311–4322.
23. H. Xin, L. M. Watson and T. N. Baker: *Acta Mater.*, 1998, **46**, 1949–1961.
24. H. Xin, C. Hu and N. Baker: *J. Mater. Sci.*, 2000, **35**, 3373–3382.
25. M. S. Selamat, T. N. Baker and L. M. Watson: *J. Mater. Process. Technol.*, 2001, **113**, 509–515.
26. J. Kaspar, A. Luft, S. Bonß and B. Brenner: Proc. Conf. on 'Nitrieren, Stickstoff im Randgefüge metallischer Werkstoffe', (ed. J. Grosch and E. J. Mittermeijer), 207–216; 2002, Aachen, AWT.
27. J. Kaspar, A. Luft, S. Bonß, B. Winderlich and B. Brenner: Proc. 10th World Conf. on 'Titanium', (ed. G. Lütjering *et al.*), 949–956; Hamburg, Germany, July 2003, DGM/Wiley-VCH Verlag GmbH & Co. KGaA.
28. U. Draugelates, R. Reiter and B. Holzmüller: Proc. Conf. on 'Reibung und verschleiß', (ed. K.-H. zum Gahr), 197–202; 1996, Bad Nauheim, DGM Informationsges.-Verl.
29. Y. Fu, H. Du and Y. Gu: *J. Mater. Eng. Perform.*, 2000, **9**, 571–578.
30. S. Bonß: 'Struktur und eigenschaften lasergaslegierter randschichten', thesis, Fraunhofer IRB Verlag, Stuttgart, Germany, 2000.
31. J. Kaspar, J. Bretschneider, B. Winderlich and B. Brenner: *Mater. Sci. Eng. A*, to be published.
32. R. Boyer, G. Welsch and E. W. Collings: 'Materials properties handbook: titanium alloys'; 1994, Materials Park, OH, ASM International.
33. J. L. Murray: 'Phase diagrams of binary titanium alloys', 176–186; 1990, Materials Park, OH, ASM International.
34. H. Rieger: 'Kavitation und tropfenschlagverschleiß'; 1977, Karlsruhe, Werkstofftechnische Verlagsgesellschaft mbH.
35. R. H. Richmann and W. P. McNaughton: *Wear*, 1990, **140**, 63–82.